Est. 1984

**ORIENTAL JOURNAL OF CHEMISTRY**
An International Open Free Access, Peer Reviewed Research Journal

www.orientjchem.org

ISSN: 0970-020 X
CODEN: OJCHEG
2015, Vol. 31, No. (4):
Pg. 1985-1997

# Density Functional Theory (B3LYP/6-311+G**) Study of Some Semicarbazones Formation Mechanism

**ABDULFATAI, A. SIAKA[1]*, UZAIRU ADAMU[2], IDRIS SULAIMAN[2] and ABBA HAMZA[2]**

[1]Department of Applied Chemistry Federal University Dutsin-ma Katsina Nigeria
[2]Department of Chemistry, Ahmadu Bello University, Zaria Kaduna Nigeria
*Corresponding author E-mail: fatsaadaby@gmail.com

http://dx.doi.org/10.13005/ojc/310416

(Received: October 28, 2015; Accepted: November 27, 2015)

**ABSTRACT**

Mechanism of formations of (E)-2-(1-phenylethylidene)hydrazinecarboxamide, 2-cyclohexyldenehydrazinecarboxamide, (Z)-2-(1-phenylpropan-2-ylidene)hydrazinecarboxamide, (Z)-2-(hexan-2-ylidene) hydrazinecarboxamide and (E)-2-((E)phenylallylidene) hydrazine-carboxamide has been investigated using density functional theory (B3LYP/6-311+G**). The mechanism was found to involve four elementary steps comprising one intermediate and two transition states. The study indicates a two-step reaction pathway, comprising an intermediate and two activated complexes for all the compounds. The mechanism involves two transition (bimolecular and unimolecular) and consecutive (bimolecular and unimolecular) schemes. The formation was found to occur sequentially; a fast pre-equilibrium between the reactants and the prereactive complex is established, followed by an internal rearrangement leading to elimination of a water molecule. The thermodynamic data were obtained for the stationary points and the kinetic study shows the unimolecular consecutive step to be the rate determining step in all the formation mechanisms. A general rate law was also established for the formation pathways.

**Key words**: pre-equilibrium, intermediate, stationary points, bimolecular and thermodynamic.

## INTRODUCTION

Nitrogen containing compounds are very widely distributed in nature and are essential to life, playing a vital role in the metabolism of all living cells. Presently, over 70 % drugs incorporate imine functionality, and these compounds owe their bioactivities to the nitrogen-containing units[1]. The most promising and convenient synthetic route for these chiral nitrogen-containing building blocks is the use of imines as electrophiles[2]. Although the synthesis of these nitrogen-containing compounds by the easily available imine is one of the most important and convenient routes, as compared with the counterpart C=O bond, C=N bond is a less explored area. This stereo selectivity of imines has been used in the synthesis of peptidic antibiotics as well as other biologically active molecules. In pharmaceutical and agro allied industries, enantio-selectivity of imines has been extensively employed,

e.g. in the synthesis of chiral herbicide (S)–Metolachlor[3]. Over the years there has been a keen interest in developing new applications of imine chemistry that enable the facile construction of the nitrogen heterocyclic frameworks found in alkaloids and other biologically active nitrogen heterocycles[4]. Semicarbazones are of much interest due to their wide spectrum of pharmacological activities, recently studies have shown that they exhibit anticonvulsant[5], analgesic, anti-inflammatory properties etc.[6]. Antipyretic activity of synthesized 4-methylphenylsemicarbazone derivatives has also been investigated by[7].

**Computational Methodology**

The geometries of the reactants, various intermediates, transition states and products were optimized using the hybrid density functional theory, i.e., Becke's three-parameter nonlocal exchange functional with the nonlocal correlation functional of Lee, Yang, Parr (B3LYP)[8]. For systems involving heavy atoms, the B3LYP/6-311+G** level of theory is a balanced choice of method for computational efficiency and accuracy, and spin contamination issue is suppressed effectively by this method[9]. Zero-point energies and harmonic vibrational frequencies were calculated at the B3LYP/6-311+G** level with the optimized geometries. The intermediates were characterized by all the real frequencies, while the transition states were characterized by one imaginary frequency. Intrinsic reaction coordinate (IRC) calculations at the B3LYP/6-311+G** level were used to confirm connections of transition state between two local minima[10]. In finding the most likely geometries of all saddle points, no arbitrary assumptions were made[11]. The energies of all the stationary points were calculated using thermochemical recipe at T1 theory level which is a composite scheme based on single-point energies, i.e., RRIMP2(FC/ 6-311++G(2df,2p)[6-311G*]. All the ab initio calculations were carried out using SPARTAN 8 and 14 packages.

## RESULTS AND DISCUSSION

In all the five system investigated, the reaction mechanism involves two transition and an intermediate elementary steps. The mechanism is a two-step reaction pathway.

**Table 1: Variations in bond distances during transformation through TSI, INT and TSII**

| TSI | Bond Length (Å) | INT | Bond Length (Å) | TSII | Bond Length (Å) |
|---|---|---|---|---|---|
| C2,C7 | 1.526 | C2,C7 | 1.540 | C2,C7 | 1.469 |
| C7,C8 | 1.523 | C7,C8 | 1.526 | C7,C8 | 1.491 |
| C7,O1 | 1.345 | C7,O1 | 1.430 | C7,O1 | 2.301 |
| O1,H10 | 1.359 | O1,H8 | 0.963 | | |
| N1,H10 | 1.206 | | | | |
| C7,N1 | 1.697 | C7,N1 | 1.484 | C7,N1 | 1.346 |
| N1,H2 | 1.021 | | | | |
| N1,N2 | 1.404 | N1,N2 | 1.397 | N1,N2 | 1.411 |

**Table 2: Variations in bond distances during transformation through TSI, INT and TSII**

| TSI | | INT | | TSII | |
|---|---|---|---|---|---|
| ∠C2C7O1 | 115.85 | | | ∠C5O1H8 | 53.10 |
| ∠C2O1H3 | 79.14 | ∠C5O1H11 | 108.39 | ∠N1H8O1 | 112.42 |
| ∠N1C2O1 | 92.13 | ∠N1C5O1 | 112.01 | ∠N1C5O1 | 71.98 |
| ∠O1H3N1 | 115.48 | ∠C5N1H8 | 111.79 | ∠C5N1H8 | 105.46 |
| | | ∠C6C5N1 | 109.58 | ∠C6C5N1 | 121.06 |
| | | ∠C4C5N1 | 108.39 | ∠C4C5N1 | 119.10 |

**Table.3: DFT B3LYP (6-311+G**) Thermodynamic parameters for acetophenone and semicarbazide reaction at 298.15 K**

| | $\Delta_f H°$ (Kj mol$^{-1}$) | S°(*Jmol$^{-1}$K$^{-1}$*) | G°(*kJ mol$^{-1}$*) | $E_e$(*kJ mol$^{-1}$*) |
|---|---|---|---|---|
| A | -86.47 | 351.05 | -1010545.65 | -1010822.21 |
| B | -107.46 | 307.13 | -736799.88 | -736937.45 |
| TSI | -221.97 | 447.25 | -1747118.51 | -1747708.73 |
| INT | -223.27 | 443.20 | -1747266.86 | -1747749.68 |
| TSII | -243.42 | 455.10 | -1747099.61 | -1747566.42 |
| P1 | +16.29 | 422.26 | -1546612.34 | -1547023.23 |
| P2 | -237.59 | 188.86 | -200732.23 | -200611.72 |

**Table 4: DFT B3LYP (6-311+G**) Calculated kinetic Parameters for acetophenone and semicarbazide reaction at 298.15 K**

| Steps | $k_2$ (*dm$^3$mol$^{-1}$s$^{-1}$*) | $k_1$ (*s$^{-1}$*) | $K_2$ | $K_1$ | A (*dm$^3$mol$^{-1}$s$^{-1}$*) |
|---|---|---|---|---|---|
| A + B→TSI | | | $7.84\times10^{-7}$ | | 4.4 |
| A+B→INT | $4.8710^{6}$ | | | | |
| INTTSII | | | | $1.4210^{4}$ | $70.6510^{12}$ |
| INTP1+P2 | | $8.8410^{16}$ | | | |

**Table 5: Variations in bond distances during transformation through TSI, INT and TSII**

| TSI | Bond Length (Å) | INT | Bond Length (Å) | TSII | Bond Length (Å) |
|---|---|---|---|---|---|
| C1,C6 | 1.527 | C1,C6 | 1.540 | C1,C6 | 1.500 |
| C5,C6 | 1.529 | C5,C6 | 1.533 | C5,C6 | 1.502 |
| C6,O1 | 1.340 | C6,O1 | 1.432 | C6,O1 | 3.617 |
| C6,N1 | 1.729 | C6,N1 | 1.473 | C6,N1 | 1.282 |
| O1H1 | 1.340 | O1H11 | 0.964 | | |
| N1,N2 | 1.404 | N1,N2 | 1.425 | N1,N2 | 1.368 |
| | | N1H13 | 1.021 | N1H13 | 1.140 |

**Table 6: Variations in bond angles during transformation through TSI, INT and TSII**

| TSI | | INT | | TSII | |
|---|---|---|---|---|---|
| ∠C5C6O1 | 115.66° | ∠C5C6O1 | 106.31° | ∠C5C6O1 | 80.08° |
| ∠C1C6O1 | 116.55° | ∠C1C6O1 | 110.26° | ∠C1C6O1 | 126.59° |
| ∠C5C6C1 | 113.32° | ∠C5C6C1 | 110.77° | ∠C5C6C1 | 116.85° |
| ∠N1C6O1 | 90.72° | ∠N1C6O1 | 112.48° | ∠N1C6O1 | 61.57° |
| ∠C5C6N1 | 108.35° | ∠C5C6N1 | 107.21° | ∠C5C6N1 | 118.86° |
| ∠C1C6N1 | 109.43° | ∠C1C6N1 | 109.73° | ∠C1C6N1 | 124.14° |
| ∠C6N1N2 | 127.19° | ∠C6N1N2 | 112.42° | ∠C6N1N2 | 130.20 ° |

**Table 7: DFT B3LYP (6-311+G**) Thermodynamic and kinetic parameters for cyclohexanone and semicarbazide reaction at 298 K**

| Species | $\Delta_f$ Ho(kJ mol$^{-1}$) | S°(Jmol$^{-1}$K$^{-1}$) | G°(kJ mol$^{-1}$) | E° (kJ mol$^{-1}$) |
|---|---|---|---|---|
| A | -224.41 | 325.60 | -813541.20 | -813856.79 |
| B | -107.46 | 307.13 | -736741.59 | -736937.45 |
| TSI | -344.85 | 426.02 | -1550121.59 | -1550626.99 |
| INT | -377.86 | 416.53 | -1550278.59 | -1550802.90 |
| TSII | -290.85 | 439.05 | -1550204.55 | -1550703.40 |
| P1 | -124.17 | 402.04 | -1349616.20 | -1350064.63 |
| P2 | -237.59 | 189.17 | -200732.49 | -200741.95 |

**Table 4: DFT B3LYP (6-311+G**) Calculated kinetic Parameters for cyclohexanone and semicarbazide reaction at 298.15 K**

| Steps | $k_2$ ($dm^3mol^{-1}s^{-1}$) | $k_1$ ($s^{-1}$) | $K_2$ | $K_1$ | A ($dm^3mol^{-1}s^{-1}$) |
|---|---|---|---|---|---|
| A+B→TSI | 67.12 dm$^3$mol$^{-1}$s$^{-1}$ | | $5.81\times10^{-4}$ | | |
| A+B→INT | | $1.71\times10^{3}$ | | | |
| INTI→TSII | $1.92\times10^{15}$ s$^{-1}$ | | | | $2.01\times10^{6}$ |
| INT→P1+P2 | | | | $2.24\times10^{11}$ | |

**Table 9: Variations in bond distances during transformation through TSI, INT and TSII benzalmethylketone and semicarbazide**

| TSI | Bond Length (Å) | INT | Bond Length (Å) | TSII | Bond Length (Å) |
|---|---|---|---|---|---|
| C9,O2 | 1.347 | C10,O2 | 1.428 | C8O2 | 2.318 |
| O2,H1 | 1.368 | O2,H19 | O.970 | | |
| C9,N1 | 1.666 | C10,N1 | 1.478 | C8N1 | 1.331 |
| N1,H1 | 1.208 | | | | |
| N1,H2 | 1.023 | N1,H10 | 1.018 | N1H2 | 1.073 |
| N1,N2 | 1.410 | N1,N2 | 1.405 | N1,N2 | 1.410 |

**Table 10: Variations in bond angles during transformation through TSI, INT and TSII benzyl methyl ketone and semicarbazide**

| TSI | | INT | | TSII | |
|---|---|---|---|---|---|
| ∠C8C9C10 | 113.91° | ∠C7C10C8 | 112.64° | ∠C7C8C9 | 120.48° |
| ∠C8C9O2 | 116.02° | ∠C8C10O2 | 106.56° | ∠C7C8O2 | 91.31° |
| ∠C10C9O2 | 115.89° | ∠C7C10O2 | 110.56° | | |
| ∠N1C9O2 | 91.85° | ∠N1C10O2 | 112.77° | | |
| ∠C9N1N2 | 126.04° | ∠C10N1N2 | 114.86° | ∠C8N1N2 | 116.48° |
| ∠C10C9N1 | 107.91° | ∠C7C10N1 | 104.54° | ∠C7C8N1 | 116.88° |
| ∠C8C9N1 | 108.32° | ∠C8C10N1 | 109.90° | ∠C8C9N1 | 121.48° |

**Table 11: DFT B3LYP (6-311+G**) Thermodynamic parameters for benzyl methyl ketone and semicarbazide reaction at 298.15 K**

| Species | $\Delta_f$ Ho(kJ mol$^{-1}$) | S°(Jmol$^{-1}$K$^{-1}$) | G°(kJ mol$^{-1}$) | E° (kJ mol$^{-1}$) |
|---|---|---|---|---|
| A | -106.21 | 370.73 | -1113712.22 | -1114057.47 |
| B | -107.46 | 307.13 | -736741.33 | -736937.45 |
| TSI | -223.17 | 464.72 | -1850294.44 | -1850833.46 |
| INT | -262.40 | 455.77 | -1850454.33 | -1851011.73 |
| TSII | -295.48 | 476.75 | -1850278.96 | -1850815.87 |
| P1 | +10.99 | 442.44 | -1649784.07 | -1650265.32 |
| P2 | -237.59 | 189.17 | -200732.23 | -200558.16 |

**Table 12: DFT B3LYP (6-311+G**) Calculated kinetic parameters for benzyl methyl ketone and semicarbazide reaction at 298.15 K**

| Steps | A | $k_2$ ($dm^3mol^{-1}s^{-1}$) | $K_2$ | $k_1$ ($s^{-1}$) | $K_1$ |
|---|---|---|---|---|---|
| A+B⇌TSI | $3.38\times10^2 dm^3mol^{-1}s^{-1}$ | | $8.6369\times10^{-4}$ | | |
| A+B→INT | | $2.1087\times10^3$ | | | |
| INTI→TSII | $2.11\times10^{14}\ s^{-1}$ | | | | $1.0508\times10^{-4}$ |
| INT⇌P1+P2 | | | | $4.8366\times10^{19}$ | |

**Table 13: Variations in bond distances during transformation through TSI, INT and TSII 2-hexanone**

| TSI | Bond Length (Å) | INT | Bond Length (Å) | TSII | Bond Length (Å) |
|---|---|---|---|---|---|
| O1,H3 | 1.378 | O1,H11 | 0.963 | | |
| C2,O1 | 1.345 | C5,O1 | 1.456 | C5,O1 | 2.362 |
| C2,C3 | 1.545 | | | | |
| C2,N1 | 1.671 | C5,N1 | 1.461 | C5,N1 | 1.327 |
| N1,H3 | 1.201 | | | N1,H8 | 1.064 |
| | | | | O1,H8 | 1.700 |

**Table 14: Variations in bond distances during transformation through TSI, INT and TSII 2-hexanone**

| TSI | | INT | | TSII | |
|---|---|---|---|---|---|
| ∠C2N1H3 | 72.22° | | | ∠C5O1H8 | 53.10° |
| ∠C2O1H3 | 79.14° | ∠C5O1H11 | 108.39° | ∠N1H8O1 | 112.42° |
| ∠N1C2O1 | 92.13° | ∠N1C5O1 | 112.01° | ∠N1C5O1 | 71.98° |
| ∠O1H3N1 | 115.48° | | | | |
| | | ∠C5N1H8 | 111.79° | ∠C5N1H8 | 105.46° |
| | | ∠C6C5N1 | 109.58° | ∠C6C5N1 | 121.06° |
| | | ∠C4C5N1 | 108.39° | ∠C4C5N1 | 119.10° |

**Table 15: DFT B3LYP (6-311+G**) Thermodynamic and kinetic parameters for 2-hexanone and semicarbazide reaction**

| Species | $\Delta_f$ Ho(kJ mol$^{-1}$) | S°(Jmol$^{-1}$K$^{-1}$) | G°(kJ mol$^{-1}$) | E° (kJ mol$^{-1}$) |
|---|---|---|---|---|
| A | -276.81 | 359.37 | -816674.47 | -817033.12 |
| B | -107.46 | 326.99 | -736800.14 | - 736937.72 |
| TSI | -392.73 | 485.61 | -1553244.62 | -1553795.19 |
| INT | -430.45 | 447.52 | -1553412.39 | - 1553982.12 |
| TSII | -366.39 | 466.88 | -1553236.48 | - 1553786.52 |
| P1 | -170.35 | 435.90 | -1352742.65 | - 1353235.19 |
| P2 | -237.59 | 189.17 | -200732.49 | - 200558.16 |

**Table 16: DFT B3LYP (6-311+G**) Calculated kinetic parameters for benzyl methyl ketone and semicarbazide reaction at 298.15 K**

| Steps | A | $k_2$ ($dm^3mol^{-1}s^{-1}$) | $K_2$ | $k_1$ ($s^{-1}$) | $K_1$ |
|---|---|---|---|---|---|
| A+B→TSI | 58.33 dm$^3$mol$^{-1}$s$^{-1}$ | | $4.12\times10^{-5}$ | | |
| A+B→INT | | $2.40\times10^{2}$ | | | |
| INTI→TSII | $17.33\times10^{13s-1}$ | | | | $2.14\times10^{5}$ |
| INT →P1+P2 | | | | $3.81\times10^{2}$ | |

**Table 17: Variations in bond distances during transformation through TSI, INT and TSII**

| TSI | Bond Length (Å) | INT | Bond Length (Å) | TSII | Bond Length (Å) |
|---|---|---|---|---|---|
| C8,C9 | 1.506 | C8,C9 | 1.497 | C8,C9 | 1.428 |
| C9,O1 | 1.404 | C9,O1 | 1.415 | C9,O2 | 2.417 |
| C9,N1 | 1.485 | C9,N1 | 1.485 | C9,N1 | 1.322 |
| N1,H2 | 2.401 | | | N1,H11 | 1.026 |
| N1,N2 | 1.405 | N1,N2 | 1.411 | N1,N2 | 1.397 |
| O1,H2 | 0.964 | O1,H9 | 0.966 | O2,H11 | 2.013 |

**Table 18: Variations in bond Angles during transformation through TSI, INT and TSII**

| TSI | | INT | | TSII | |
|---|---|---|---|---|---|
| ∠C7C8C9 | 125.11° | ∠C7C8C9 | 123.19 | ∠C7C8C9 | 127.57 |
| ∠C8C9O1 | 109.83° | ∠C8C9O1 | 108.34 | ∠C8C9O2 | 123.84 |
| ∠N1C9O1 | 110.00° | ∠N1C9O1 | 106.08 | ∠N1C9O2 | 79.17 |
| ∠C8C9N1 | 113.30° | ∠C8C9N1 | 114. 53 | ∠C8C9N1 | 130.14 |
| ∠C9N1H2 | 53.70° | | | | |
| ∠C9N1H10 | 109.70° | ∠C9N1H11 | 108.71 | ∠C9N1H11 | 111.52 |
| ∠C10N2N1 | 120.13° | ∠C10N2N1 | 118.14 | ∠C10N2N1 | 120.53 |
| | | ∠C9N1N2 | 112.74 | ∠C9N1N2 | 122.50 |

**Table 19: DFT B3LYP (6-311+G**) Thermodynamic and kinetic parameters for cinnamaldehyde and semicarbazide reaction**

| Species | $\Delta_f$ Ho(kJ mol$^{-1}$) | S°(Jmol$^{-1}$K$^{-1}$) | G°(kJ mol$^{-1}$) | E° (kJ mol$^{-1}$) |
|---|---|---|---|---|
| A | +20.11 | 364.06 | -1110542.45 | -1110830.99 |
| B | -107.46 | 326.99 | -736799.88 | -736937.45 |
| TSI | -97.49 | 448.26 | -1847275.64 | -1847747.96 |
| INT | -121.49 | 449.87 | -1847271.44 | -1847769.76 |
| TSII | -143.60 | 455.99 | -1847145.94 | -1847711.47 |
| P1 | +114.47 | 435.43 | -1646629.26 | -1647051.71 |
| P2 | -237.59 | 188.86 | -200732.49 | -200741.95 |

**Table 16: DFT B3LYP (6-311+G**) Calculated kinetic parameters for Cinnamaldehyde and semicarbazide reaction at 298.15 K**

| Steps | A | $k_2$ ($dm^3mol^{-1}s^{-1}$) | $K_2$ | $k_1$ ($s^{-1}$) | $K_1$ |
|---|---|---|---|---|---|
| A+B⇌TSI | 9.5441 $dm^3mol^{-1}s^{-1}$ | | $2.1710\times10^{-14}$ | | |
| A+B→INT | | $7.7197\times10^{2}$ | | | |
| INTI⇌TSII | $3.5232\times10^{13}s^{-1}$ | | | | $2.4582\times10^{9}$ |
| INT→P1+P2 | | | | $9.6855\times10^{16}$ | |

The general reaction mechanism for reaction between acetophenone and semicarbazide is as presented in Figure 1 below.

In the transition state reaction scheme, the first step involving C=O, N–H partial cleavage, C–N and O–H partial bonding is found to have activation energy of 50 *kJ/mol*. This in turn forms the intermediate through an endothermic (+27 *kJ/mol*)[12] and non-spontaneous step (+79 *kJ/mol*) in Figures 2 and 3 respectively. Next the intermediate, through intra-molecular interaction, in turn forms the second transition state (TSII) which eventually disappears to form the products. This endothermic and non-spontaneous transformation is accomplished through C=N, O–H bond formation and N–H bond cleavage with energy barrier of 187 *kJ/mol* as seen respectively in Figures 2 and 3 below. The two-step reaction mechanism presented by the potential and free energies profiles shows that the overall transformation is endothermic (+122 *kJ/mol*) and slightly non-spontaneous (+1 *kJ/mol*). The first consecutive (bimolecular) step is found to be the rate determining step. The geometrical variations of the transition states and intermediate during the course of reaction are as presented in Tables 1 and 2 below, while Tables 3 and 4 respectively show thermodynamic and kinetic parameters for the reaction.

It can be seen that there is an increase of about 0.014Å in C2-C7 bond length as the reaction proceeds from TS1 to INT, while the same bond length decreases by 0.071 Å proceeding from INT to TSII. Similar trend was observed in C7-C8 bond order as the reaction progresses from the first transition state through intermediate to the second transition state. However, there is a progressive increase in bond length (for C7-O1) from the first transition state to the second transition state in the magnitude of 0.085 at intermediate and 0.871 at TSII in readiness for C7-O1 bond fission in the final product. In the same vein, C7-N1 bond length experiences decrease progressively from TSI through INT to TSII (with 0.213 from TSI to INT and 0.138 from INT to TSII) characteristic of double bond. It can also be seen that N1-N2 remains almost unchanged as it is relatively far away from the reactive site. Similar trends were also observed in bond angles as the molecules undergo transformation through the stationary points to the product.

The general reaction mechanism for reaction between cyclohexanone and semicarbazide is as presented in Figure 4 below.

The bimolecular transition step leading to the first activated complex (TSI) is computed to be non-spontaneous (161 *kJ/mol*) Figure 6 belowe. This transition is accomplished through intermolecular engagement involving C=O bond partial cleavage, O–H and C–N partial bond formation. It's also associated with very high energy barrier of 168 *kJ/mol*. The pre-exponential factor and equilibrium values are very small as only few of the reacting molecules is energized enough to overcome the activation energy for this step. The TSI then forms slightly less stable (relative to the two reacting molecules) intermediate [13]. The bimolecular consecutive step slightly non-spontaneous and exothermic (+4 *kJ/mol* and –8 *kJ/mol* respectively, it is found to be the rate determining step the value of which is presented in Table below. The resulting intermediate further undergoes intra-molecular interaction through second transition state (TSII) involving C=N partial formation and C–O and H–N partial cleavage as presented in the Table below to form the products. The products (P1+P2) has stabilization energy of (–66 *kJ/mol*) relative to the starting molecules, indicating that the two-step mechanism is largely spontaneous and slightly exothermic by –12 *kJ/mol*. The unimolecular consecutive step has barrier height of 99 *kJ/mol*,which makes it much faster than the preceding bimolecular consecutive step. The geometrical variations of the transition states and intermediate during the course of reaction are as presented in Tables 5 and 6 below, while Tables 7 and 8 respectively show thermodynamic and kinetic parameters for the reaction.

One observes that as the reaction proceeds from first transition state to the intermediate, C1-C6 bond length increases by 0.013 Å, but decreases by 0.040 Å on getting to the second transition state. C5-C6 bond length was found to

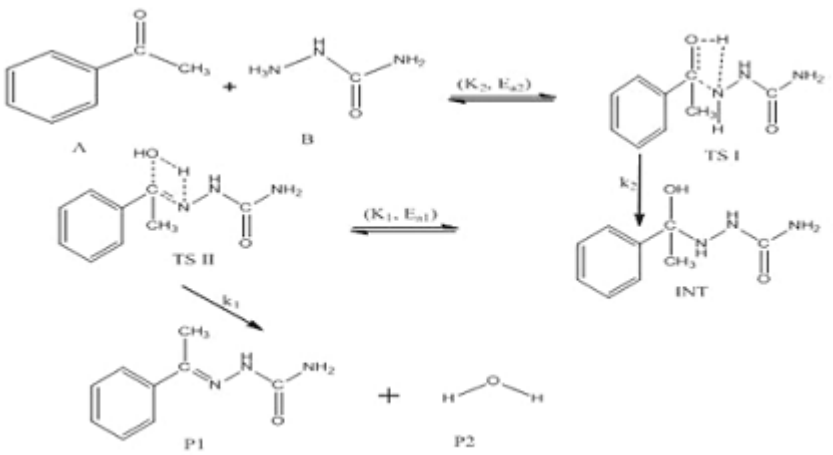


**Fig. 1: General reaction scheme between acetophenone and semicarbazide**

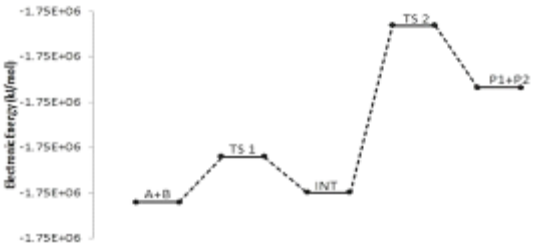


**Fig. 2: Profiles of the potential energy surface for acetohenone and semicarbazide reaction**


**Fig. 3: Profiles of the Gibbs free energy for acetohenone and semicarbazide reaction.**

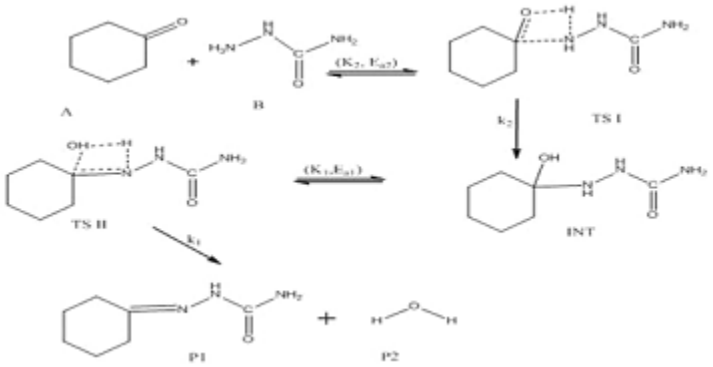


**Fig. 4: General reaction scheme between cyclohexanone and semicarbazide**

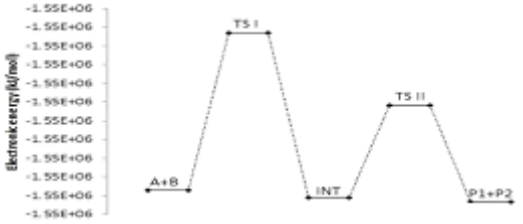


**Fig. 5: Profiles of the potential energy surface for cyclohexanone and semicarbazide reaction**

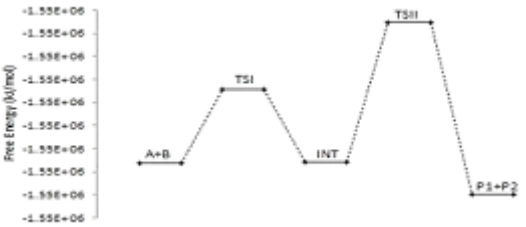


**Fig. 6: Profiles of the Gibbs free energy for cyclohexanone and semicarbazide reaction**

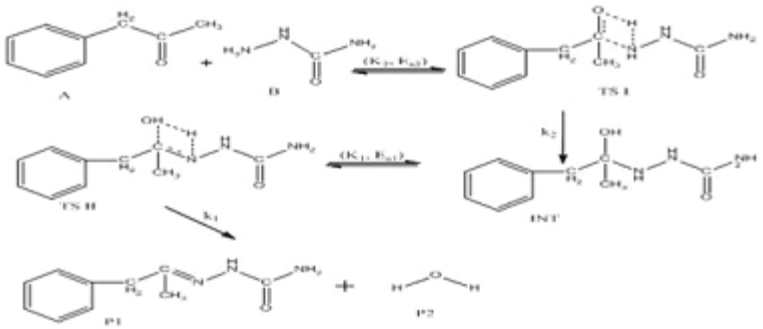


**Fig. 7: General reaction scheme between benzyl methyl ketone and semicarbazide**

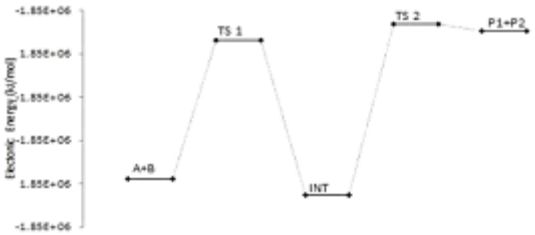


**Fig. 8: Profiles of the potential energy surface for benzyl methyl ketone and semicarbazide reaction**

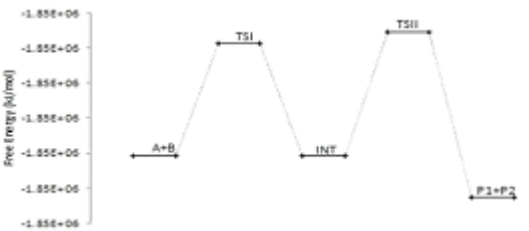


**Fig.9: Profiles of the Gibbs free energy for benzyl methyl ketone and semicarbazide reaction**

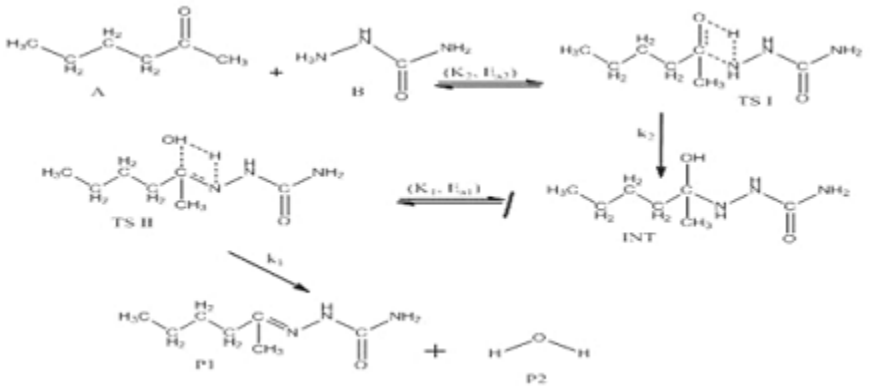


**Fig.10: General reaction scheme between 2-hexanone and semicarbazide**

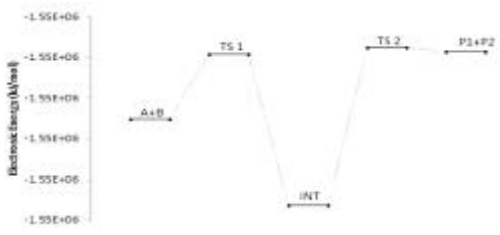


**Fig. 11: Profiles of the potential energy surface for 2-hexanone and semicarbazide reaction**

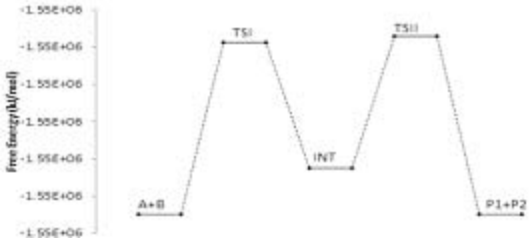


**Fig. 12: Profiles of the Gibbs free energy for 2-hexanone and semicarbazide reaction**

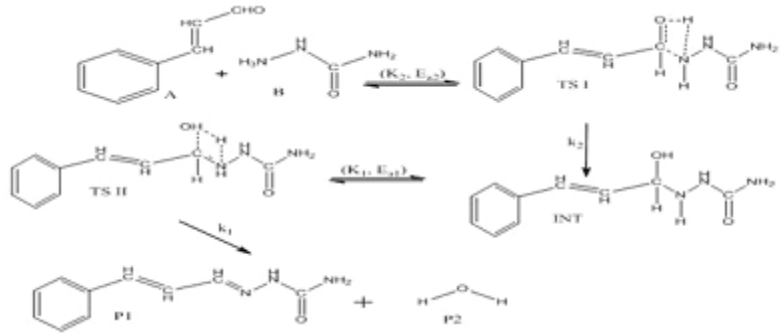


**Fig. 13: General reaction scheme between 2-hexanone and semicarbazide**

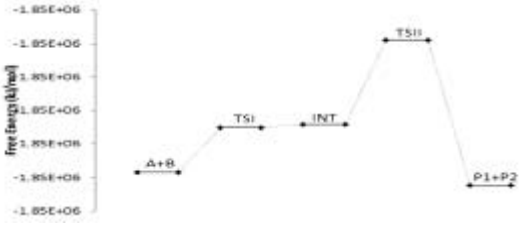


**Fig.14: Profiles of the potential energy surface for cinnamaldehyde and semicarbazide reaction**


**Fig.15: Profiles of the Gibbs free energy for cinnamaldehyde and semicarbazide reaction**

undergo similar variations as the reaction progresses from TSI through INT to TSII. It was also seen that C6-O1 bond order experiences increase progressively from TSI to TSII preparatory for the bond fission in the final product. C6-N1 bond length progressively decreases by 0.256° at INT and 0.191° at TSII leading to double bond formation in the final product[14]. While the bond angle ∠C5C6O1 decreases by 35.58°, ∠C1C6O1 increases by 10.04° as the system transforms from TSI to TSII. Similar increases were seen for ∠C5C6N1, ∠C5C6N1 and ∠C6N1N2, moving from TSI through INT to TSII.

The benzyl methyl ketone and semicarbazide through hydrogen abstraction O–H and C–N bond forms an activated complex (with un-stability of +159 *kJ/mol*). This transition state disappears to form a more stable (–1 *kJ/mol* and –160 *kJ/mol* compared to the starting molecules and the transition state TSI respectively) intermediate. This transformation of the reactants to intermediate has a barrier height of 160 *kJ/mol*. The intermediate in turn form the respective semicarbazone via a second activated complex with activation energy and relative stability of 197 *kJ/mol* and –59 *kJ/mol*. The energetics of the general reaction suggest indicates that the overall mechanism is moderately spontaneous (–60 *kJ/mol*) but largely endothermic (170 *kJ/mol*). The energetics (electornic and free) of the overall mechanism are presented in Figures 8 and 9 respectively. Kinetically, the rate determining step is found to be the bimolecular consecutive step. The geometrical variations of the transition states and intermediate during the course of reaction are as presented in Tables 9 and 10 below, while Tables 11 and 12 respectively show thermodynamic and kinetic parameters for the reaction.

Eventual break off of C-O bond in the final product was indicated as the bond length increases by 0.971 Å from the first transition state (TSI) to the second transition state (TSSII). However characteristic C=N bond formation[15] was shown as the bond length decreases progressively by 0.335 at TSII. Meanwhile, N1-N2 bond order was observed to remain unchanged being distant from active center. While ∠C8C9C10 alternates by -1.27° at INT and by 7.84° at TSII, ∠C8C9O2 decreases continuously by 9.46° at INT and by 15.25° at TSII.

The first activated complex (TS1) formation appears to be exothermic and non-spontaneous with a barrier height of (176 *kJ/mol*). This step has equilibrium value for this step suggest that only very few reacting molecules actually pre-aggregate to form the activated complex, necessitating the need for reaction condition adjustment for forward equilibrium. The transition state proceeds to form the intermediate (INT) through O–H single bond formation, C–N single bond formation, C=O bond cleavage and N–H single bond cleavage, with their corresponding bond length and bond angle shown in the Table below. The intermediate has lower stabilization energy of (168 *kJ/mol*) than the activated complex TS1 as shown in Figure 12 below. The intermediate, by intra-molecular interaction through C=N and O–H bond formation leads to second activated complex TS II. This intra-molecular step is both exothermic by (–106 *kJ/mol*) and non-spontaneous by +62 *kJ/mol*, with some reasonable equilibrium value and energy height of 80 *kJ/mol* (Figure 11) [16]. Finally, through C–O bond cleavage and subsequent dehydration, the transition state (TSII) forms the products (semicarbazone and water). The two consecutive steps are competing for the reaction rate determination, but the bimolecular (first) step manage to be the rate determining step, since the higher the rate constant value the faster the reaction[17].

The general reaction mechanism for reaction between cinnamaldehyde and semicarbazide is as presented in Figure 13 below.

The cinnamaldehyde and semicarbazide interact through C–N, O–H bond formation and C–O bond cleavage to form TS1 with barrier height of about 21 *kJ/mol* compared to the starting molecules. The activated complex TSI is less stable than the two molecules A and B by (67 *kJ/mol*). This intermolecular engagement leads to intermediate with stabilization energy of 4 *kJ/mol*. The step (consecutive) leading to the intermediate formation is e-thermic and non-spontaneous with +71 *kJ/mol* free energy and very low equilibrium which suggests that input (in form of energy) is required to shift the reaction equilibrium forward. Again the intermediate undergoes intra-molecular interaction through C–N and O–H bond formation to form the

second activated complex (TSII) which has an energy barrier of 58 *kJ/mol* but with appreciable equilibrium constant. The second transition state is highly unstable by 126 *kJ/mol* compared to the intermediate from which it was formed. The second activated complex TSII eventually forms the major product and the leaving water molecules with high stabilization energy of (–216 *kJ/mol*). Free energy and potential energy reaction profiles (Figures 14 and 15) suggest a two-step mechanism involving two transition states and an intermediate, and the overall is slightly spontaneous by –19 *kJ/mol* and exothermic by – 25 *kJ/mol*. The geometrical variations of the transition states and intermediate during the course of reaction are as presented in Tables 9 and 10 below, while Tables 11 and 12 respectively show thermodynamic and kinetic parameters for the reaction. The geometrical variations of the transition states and intermediate during the course of reaction are as presented in Tables 17 and 18 below, while Tables 19 and 20 respectively show thermodynamic and kinetic parameters for the reaction.

C8-C9 bond length decreases, while C9-O1 bond order increases progressively characteristic of bond fission in the final product. Again double bond order characteristic of C=N in the product was indicated by the continuous bond decrease from TSI through INT to TSII. Also worth mentioning is the O-H bond stretching by 1.049 Å preparatory to its cleavage in the final product. Similar variations were also observed in bond angles as the system undergoes transformation through TSI, INT and TSII to the final product.

**Mechanism and Rate Law of the Reaction**

Below are the elementary steps making the formation mechanism:

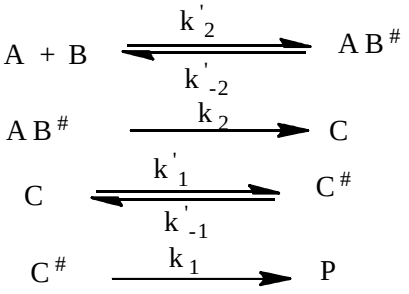


The rate laws for all the products of the reaction can be written as follow:

$$\frac{d[P]}{dt} = k_1[C^{\#}] \quad \text{(i)}$$

$$\frac{d[C^{\#}]}{dt} = -k_1[C^{\#}] - k'_{-1}[C^{\#}] + k'_1[C \quad \text{(ii)}$$

$$\frac{d[C]}{dt} = -k'_1[C] + k'_{-1}[C^{\#}] + k_2[AB^{\#}] \quad \text{(iii)}$$

$$\frac{d[AB^{\#}]}{dt} = -k_2[AB^{\#}] - k'_{-2}[AB^{\#}] + k'_2[A][B] \quad \text{(iv)}$$

Using steady state approximation, from equation (ii)

$$[C^{\#}] = \frac{k'_1}{k_1 + k'_{-1}}[C] \quad \text{..(v)}$$

Using equations (iii) and (v), we have

$$[C] = \frac{k_2(k_1 + k'_{-1})[AB^{\#}]}{k'_1 k_1} \quad \text{...(vi)}$$

Similarly, from equation (iv), we have,

$$[AB^{\#}] = \frac{k'_2}{k_2 + k'_{-2}}[A][B] \quad \text{...(vii)}$$

Equations (vi) and (vii) gives,

$$[C] = \frac{k_2 k'_2 (k_1 + k'_{-1})}{k'_1 k_1 (k_2 + k'_{-2})}[A][B] \quad \text{...(viii)}$$

From equations (viii) and (v), we have,

$$[C^{\#}] = \frac{k_2 k'_2}{(k_2 + k'_{-2})}[A][B] \quad \text{...(ix)}$$

Therefore the overall rate law can be written as;

$$\frac{d[P]}{dt} = \frac{k_2 k'_2}{(k_2 + k'_{-2})}[A][B] \quad \text{...(x)}$$

where $\frac{k_2 k'_2}{(k_2 + k'_{-2})} = K'$, experimental rate constant.

## CONCLUSION

Formation mechanisms of five semicarbazones have been investigated at B3LYP (6-311+G**) theory level. The bimolecular consecutive was found to be the rate determining step except in the (Z)-2-(hexan-2-ylidene)hydrazinecarboxamide formation mechanism where both the bimolecular and unimolecular consecutive steps were found to be competing ($k_2$ = 2.40×$10^2$ $dm^3mol^{-1}s^{-1}$ and $k_2$ = 3.8110$^2$ $s^{-1}$), with the bimolecular still becoming the rate determining step and the unimolecular step the fastest. During the course of transformation through the first transition state (TS1), intermediate and second transition state (TS2) to the product geometrical (bond lengths and bond angles) variations alongside bond cleavage and bond formation were observed.

**Authors' contributions**

AAS carried out the total experimental work under the guidance of UA. SD performed the data analysis, while HA prepared all the JPEG files, with AAS drafting the manuscript. All authors read and approved the final manuscript.

## ACKNOWLEDGEMENTS

The authors are grateful to the head of the department of chemistry of Ahmadu Bello University for systemic support through the provision of dedicated power source.

**Competing interests**

The authors declare that they have no competing interests.

## REFERENCES

1. Liu, G., Cogan, O. A., Ellman, J. A., *J. Amer. Chem. Soc*. 1997, *119*: 9913-9914
2. Kleinman, E. F., Chapter 4. In: *Comprehensive Organic Synthesis,* 3rd ed., Trost, B. M.; Fleming, I. (eds.), Pergamon Press, Oxford, **1991**, Vol. 2, p. 893).
3. Blaser, H. U., Pugin, B., Spinder, F., Togni, A., *Comp. Rend. Chim.* **2002**, *5*: 379-385
4. Rudolph A. C., Machauer R., and Martin S. F., *Tetrahedron Letters* **2004**; *45*: 4895.
5. Pandeya, S. N., Mishra, V.;,Ponnilavarasan, I.;,Stables, J. P., *Pol. J. Pharmacol.*, **2000**, *52*, 283.
6. Singh, H. P., Chauhan, C. S., Pandeya, S. N., Sharma C. S., Srivastava B. and Singhal M.,. *Der. Pharm. Lett*. **2010**, *2*: 460-462.
7. Singhal, M. and A. Paul, *Global J. Pharmacol*., **2011b,** *5*, 60-66.
8. Becke A. D., *J. Chem. Phys.* **1993**, *98*, 5648 (b) Lee C., Yang. W., Parr. R. G., *Phys.* Rev. B; *Condens.* Matter Mater. Phys. **1988**. *3,* 785.
9. Huang W., Jicun L., Xinli S., Yuzhen L., Hua H., Baoshan W., Hongmei S. and Fanao K. *J. Phys. Chem. A* ***2006****, 110,* 10336 – 10344
10. Gonzalez, C.; Schlegel, H. B. *J. Phys. Chem.***1969**. *90,*2154.
11. Hideo, T., Hakuai, I., Masato M. I., *J. Comput. Chem. Jpn.,* 2003, *2(4),* 127-134.
12. Shabaan A. K. E., and Saadullah G. A., *Chemistry Central Journal* **2011**, *5*: 66
13. Isamu S., Tadafumi U., Mitsuru S., Hideaki K., Hiroyuki O and Yujiro H. *Organic Letters* **2006,** *8(6),* 1041-1044
14. Hideo T., Hakuai I and Masato M. I. *J. Comput. Chem. Jpn* **2003**, 2(4); 127-134.
15. G.S. Hammond. *J. Am.chem. Soc.* **1955**, *77*, 334.
16. Robert C. M., Heidi M. M., and Peslherbe G. H., *Can. J. Chem.* **2005**, *83*; 1615-1625.
17. Szajewski R. P. and Whitesides G. M. *Journal of the American Chemical Society*, **1980**, *102(6),* 2011–2026.